

**EVALUATING INTERFRACTION MOTION
THRESHOLDS IN IMAGE-GUIDED
RADIOTHERAPY (IGRT) FOR LUNG AND SPINE
STEREOTACTIC BODY RADIOTHERAPY (SBRT)**

LAU EN XIN

**SCHOOL OF HEALTH SCIENCES
UNIVERSITI SAINS MALAYSIA**

2025

**EVALUATING INTERFRACTION MOTION
THRESHOLDS IN IMAGE-GUIDED
RADIOTHERAPY (IGRT) FOR LUNG AND SPINE
STEREOTACTIC BODY RADIOTHERAPY (SBRT)**

by

LAU EN XIN

**Dissertation submitted in partial fulfilment of the requirements
for the degree of
Bachelor in Medical Radiation (Honours)**

July 2025

CERTIFICATE

This is to certify that the dissertation entitled “EVALUATING INTERFRACTION MOTION THRESHOLDS IN IMAGE-GUIDED RADIOTHERAPY (IGRT) FOR LUNG AND SPINE STEREOTACTIC BODY RADIOTHERAPY (SBRT)” is the bona fide record of research work done by Ms LAU EN XIN during the period from October 2024 to July 2025 under my supervision. I have read this dissertation and that in my opinion it conforms to acceptable standards of scholarly presentation and is fully adequate, in scope and quality, as a dissertation to be submitted in partial fulfillment for the degree of Bachelor in Medical Radiation (Honours).

Main supervisor,



.....
Dr. Jayapramile A/P Jayamani

Lecturer

School of Health Sciences

Universiti Sains Malaysia

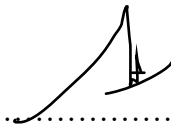
Health Campus

16150 Kubang Kerian

Kelantan, Malaysia

Date: 27 July 2025.....

Field supervisor,



.....
En. Reduan Bin Abdullah

Medical Physicist

Department of Nuclear Medicine,

Radiotherapy & Oncology

Hospital Pakar Universiti Sains

Malaysia

16150 Kubang Kerian

Kelantan, Malaysia

Date: 27 July 2025.....

DECLARATION

I hereby declare that this dissertation is the result of my own investigations, except where otherwise stated and duly acknowledged. I also declare that it has not been previously or concurrently submitted as a whole for any other degrees at Universiti Sains Malaysia or other institutions. I grant Universiti Sains Malaysia the right to use the dissertation for teaching, research and promotional purposes.



.....
LAU EN XIN

Date: 27 July 2025

ACKNOWLEDGEMENT

First and foremost, I would like to express my heartfelt gratitude to my main supervisor, Dr. Jayapramila A/P Jayamani, lecturer at the School of Health Sciences, Universiti Sains Malaysia, for her invaluable guidance, continuous support and encouragement throughout the course of this research. Her expertise, insightful feedback and dedication to academic excellence have greatly contributed to the successful completion of this thesis. I am truly grateful for her patience, constructive advice and generous mentorship throughout this journey.

I would also like to extend my sincere appreciation to my field supervisor, En. Reduan Bin Abdullah, medical physicist at the Department of Nuclear Medicine, Radiotherapy & Oncology, Hospital Pakar Universiti Sains Malaysia, for his kind assistance and cooperation during my data collection at the department. His support and facilitation were crucial in ensuring the smooth execution of the data collection process.

My gratitude also goes to the staff of the Department of Nuclear Medicine, Radiotherapy & Oncology for their collaboration and to all individuals who contributed directly or indirectly to this research project. Finally, I wish to thank my family and friends for their constant encouragement, understanding and emotional support throughout this academic journey.

TABLE OF CONTENTS

CERTIFICATE	ii
DECLARATION	iii
ACKNOWLEDGEMENT	iv
TABLE OF CONTENTS	v
LIST OF TABLES	viii
LIST OF FIGURES	x
LIST OF SYMBOLS	xiv
LIST OF ABBREVIATIONS	xvi
LIST OF APPENDICES	xx
ABSTRAK	xxi
ABSTRACT	xxiii
CHAPTER 1 INTRODUCTION	1
1.1 Study Background.....	1
1.2 Problem Statement	4
1.3 Research Objectives	6
1.3.1 General Objective.....	6
1.3.2 Specific Objectives.....	6
1.4 Significance of Study	6
CHAPTER 2 LITERATURE REVIEW	8
2.1 Tumour Motion	8
2.2 Computed Tomography (CT) Simulation for Motion Assessment.....	11
2.2.1 Slow CT	12
2.2.2 Four-dimensional CT (4DCT).....	14
2.3 Radiotherapy Treatment Planning Techniques	15
2.3.1 Target Volume Definitions.....	17

2.4	Stereotactic Body Radiotherapy (SBRT)	18
2.5	Interfraction Motion	21
2.6	Image-guided Radiotherapy (IGRT) Techniques for Motion Management ..	22
2.6.1	kV-Cone Beam Computed Tomography (kV-CBCT)	23
2.7	Tolerance Thresholds for Interfraction Motion in SBRT.....	24
2.7.1	AAPM Task Group 142 Quality Assurance (QA) Standards	25
2.7.2	Other Guidelines	25
CHAPTER 3 METHODOLOGY.....		28
3.1	Materials.....	28
3.1.1	Orfit Vacuum Bag	28
3.1.2	Philips Brilliance CT Big Bore	29
3.1.2(a)	Philips Bellows	30
3.1.3	ArcCHECK Phantom	31
3.1.4	Varian Clinac iX Linear Accelerator	32
3.1.4(a)	On-Board Imager 1.6 2015 by Varian Medical Systems.....	33
3.1.5	Eclipse Treatment Planning System.....	35
3.1.6	IBM Statistical Package for Social Science (SPSS) Software	36
3.2	Methods.....	37
3.2.1	JEPeM Ethical Approval.....	37
3.2.2	Patient Selection.....	38
3.2.3	CT Simulation	38
3.2.3(a)	CT Simulation for Lung SBRT.....	38
3.2.3(b)	CT Simulation for spine SBRT.....	42
3.2.4	Measurement of Tumour Motion in 4D-Gated Slow CT Simulation	43
3.2.5	SBRT Treatment Planning	46
3.2.5(a)	Contouring	46

3.2.5(b)	SBRT Treatment Planning Technique.....	48
3.2.5(c)	SBRT Plan Evaluation.....	50
3.2.6	Patient-Specific Quality Assurance (PSQA) for SBRT	51
3.2.7	SBRT Treatment Delivery	53
3.2.7(a)	kV-CBCT IGRT Verification.....	54
3.2.8	Interfraction Motion Assessment	56
3.2.9	Evaluation of Threshold refer to AAPM TG-142	57
3.2.10	Statistical Analysis	58
3.2.10(a)	Analysis of Average GTV Volume	58
3.2.10(b)	Tumour Motion Analysis and Correlation with Average GTV Volume.....	58
3.2.10(c)	Analysis of Interfraction Motion Displacement	59
3.3	Study Flowchart	60
CHAPTER 4 RESULTS AND DISCUSSION		61
4.1	Patient Demographics and Clinical Characteristics	61
4.2	Analysis of Average GTV Volume.....	65
4.3	Tumour Motion Analysis and Correlation with Average GTV Volume	67
4.4	Analysis of Interfraction Motion Displacement in Lung and Spine SBRT ...	72
4.4.1	Analysis of Interfraction Motion Displacement across Fractions.....	77
4.4.2	Comparison of Interfraction Motion by Simulation Technique.....	79
4.5	Evaluation of Threshold refer to AAPM TG-142	80
4.6	Limitations	84
CHAPTER 5 CONCLUSIONS		86
5.1	Conclusions	86
5.2	Recommendations for Future Research	87
REFERENCES.....		88
APPENDICES		

LIST OF TABLES

		Page
Table 2.1	Tumour motion magnitudes in lung and spine referring to published work.....	10
Table 2.2	Target volume definitions based on ICRU Report 83. (Adapted from Grégoire and Mackie, 2011).....	17
Table 2.3	The 4 Rs of radiobiology in SBRT. (Adapted from Qiu et al., 2020).....	19
Table 2.4	Comparison between conventional radiotherapy and SBRT. (Adapted from Benedict et al., 2010).....	21
Table 2.5	Interfraction Motion Tolerances in SBRT referring to published work.. ..	26
Table 3.1	Dosimetric properties of Orfit vacuum bag.	29
Table 3.2	Inclusion and exclusion criteria for this study.	38
Table 3.3	Anatomical landmarks for lung SBRT simulation, including superior (Sup), medial (Med), right lateral (Rt Lat), left lateral (Lt Lat) and inferior (Inf).....	39
Table 3.4	General CT acquisition parameters for SBRT simulation.	40
Table 3.5	Anatomical landmarks for spine SBRT simulation, , including superior (Sup), medial (Med), right lateral (Rt Lat), left lateral (Lt Lat) and inferior (Inf).....	43
Table 3.6	Summary of SBRT treatment planning technique.	48
Table 3.7	Dose optimisation objectives and priorities for SBRT treatment planning.....	49
Table 3.8	Summary of dose constraints for SBRT treatment plan.....	50
Table 3.9	OARs dosimetric limits for lung and spine SBRT. (Adapted from Kong et al., 2011).....	51

Table 3.10	Parameters for kV-CBCT acquisition in SBRT.....	55
Table 4.1	Patient demographics and clinical characteristics.....	62
Table 4.2	Comparison of average GTV volume between lung SBRT and spine SBRT using Mann-Whitney U test ($p < 0.05$).....	65
Table 4.3	Spearman's rank correlation between volume of average GTV and tumour motion in X, Y and Z axes for maximum and minimum phases in lung SBRT patients who underwent 4D-gated slow CT simulation ($n = 7$; $p < 0.05$).....	68
Table 4.4	Descriptive statistics of the mean interfraction motion displacements between lung SBRT ($n = 14$) and spine SBRT ($n = 4$) across all axes. Translational displacements are expressed in mm and rotational displacements in degrees ($^{\circ}$).....	73
Table 4.5	Comparison of displacement of interfraction motion across fractions in lung ($n = 14$) and spine ($n = 4$) SBRT using Friedman test ($p < 0.05$).....	78
Table 4.6	Comparison of interfraction motion between 4D-gated slow CT ($n = 7$) and standard helical CT ($n = 7$) simulation techniques in lung SBRT patients using Mann–Whitney U test ($p < 0.05$).....	79
Table 4.7	Interfraction motion evaluated against AAPM TG-142 threshold. The n refers to the number of patients. The range refers to the minimum and maximum mean interfraction motion displacements observed in lung SBRT ($n = 14$) and spine SBRT ($n = 4$) across all axes.....	81

LIST OF FIGURES

	Page
Figure 1.1 Comparison of dose distribution between 3D-CRT and SBRT treatment planning techniques for lung treatment. The SBRT plan demonstrates a steeper dose fall-off than the 3D-CRT plan. (Adapted from Ohtaki et al., 2019).....	2
Figure 2.1 Workflow of radiotherapy.....	8
Figure 2.2 The (A) Abdominal pressure belt and (B) pressure gauge for motion management. (Adapted from Yorke et al., 2015).....	12
Figure 2.3 The (a) axial, (b) sagittal and (c) coronal views showing the projection of ITV _{all} (blue) and ITV _{all+slow} (red) on a modified slow CT scan, comparing between both volumes. (Adapted from Jang et al., 2014)	13
Figure 2.4 Pixel-based intensity projection techniques used in 4DCT, including (a) separate phases of the 4DCT, (b) MIP and (c) AIP. (Adapted from Underberg et al., 2005).....	15
Figure 2.5 Comparisons in the beam arrangements between VMAT (left) and 3D-CRT (right). (Adapted from Saito et al., 2023)	16
Figure 2.6 Definition of volumes as per ICRU Report 83: GTV in red, CTV in green, ITV in blue, PTV in grey, treated volume and irradiated volume. (Adapted from Grégoire and Mackie, 2011).....	18
Figure 2.7 Example of the isodose distribution of a 55 Gy in five fractions of 11 Gy lung SBRT. (Adapted from Kinj et al., 2022).....	20
Figure 2.8 Superior-inferior (red), anterior-posterior (green) and lateral (blue) directions.	22
Figure 3.1 Orfit vacuum bag.....	29
Figure 3.2 Brilliance CT Big Bore.	30
Figure 3.3 Philips bellows.	31

Figure 3.4	ArcCHECK phantom.	32
Figure 3.5	Varian Clinac iX linear accelerator.....	33
Figure 3.6	On-Board Imager 1.6 2015 by Varian Medical Systems.	34
Figure 3.7	Interface of Eclipse TPS.....	36
Figure 3.8	Interface of IBM SPSS Software v.29.0.	37
Figure 3.9	Setup of the patient on the vacuum bag with bellows system during CT simulation for lung SBRT. (Adapted from Philips CT Clinical Science, 2013).....	39
Figure 3.10	Respiratory waveform generated during 4D-gated CT simulation. The green cross indicates the location selected for motion tracking (left) while the respiratory waveform (right) represents the patient's breathing cycle used to synchronise CT image acquisition with specific respiratory phases.	41
Figure 3.11	Respiratory cycle sorting in 4D-gating, divided into ten phases (0%–90%), with approximately 130 CT images reconstructed per phase.....	41
Figure 3.12	Workflow of CT simulation procedure.....	42
Figure 3.13	Respiratory phase display in Eclipse TPS, showing all ten phases from 0% to 90%. The maximum (max) and minimum (min) phases were selected for motion evaluation and used in generating the average GTV.	44
Figure 3.14	4D-gated slow CT simulation images of lung SBRT in (a) axial, (b) sagittal and (c) coronal views. The yellow contour represents the GTV delineated at phase 0% (maximum) while the red contour represents the average GTV generated from the accumulated phase dataset.....	44
Figure 3.15	Tumour motion measurement visualised in (a) axial, (b) sagittal and (c) coronal views. The green arrows indicate the direction of tumour motion: (a) Z direction, (b) Y direction and (c) X direction.	45

Figure 3.16	Example of a lung SBRT treatment plan created using VMAT. The figure shows isodose distributions and the associated DVH. The PTV is covered with a conformal high-dose region while the DVH demonstrate dose sparing for critical structures.....	46
Figure 3.17	Target and OAR contouring for a lung SBRT case, including GTV (purple), ITV (red), PTV (pink) and OARs. (Adapted from Adebahr et al., 2015).....	47
Figure 3.18	Target and OAR contouring for a thoracic spine SBRT case, including CTV, PTV, spinal cord, oesophagus and heart. (Adapted from Lideståhl et al., 2023).....	47
Figure 3.19	R50% ring structure.	50
Figure 3.20	Setup of PSQA using ArcCHECK phantom and cylindrical ionisation chamber.	52
Figure 3.21	Acquisition of kV-CBCT scan using the OBI integrated with the Varian Clinac iX linear accelerator for IGRT in SBRT. (Adapted from Zhang, 2013)	54
Figure 3.22	Matching of kV-CBCT and planning CT images using OBI by Varian Medical Systems. (Adapted from Wang et al., 2012)	56
Figure 3.23	Interfraction motion assessment using Eclipse TPS. The figure displays recorded couch displacement data in the vertical (Vrt), longitudinal (Lng) and lateral (Lat) directions, along with rotational (Rtn) deviations, for each treatment fraction.	57
Figure 3.24	Study flowchart illustrating the SBRT treatment workflow and interfraction motion analysis for evaluating interfraction motion thresholds in IGRT for lung and spine SBRT.....	60
Figure 4.1	Boxplot of GTV volume between lung and spine SBRT. Lung tumours exhibit a wider range and include a notable outlier (477.20 cm ³) whereas spine tumours show a more consistent distribution with a higher median GTV.....	65
Figure 4.2	Boxplot of tumour motion in X (lateral), Y (superior-inferior) and Z (anterior-posterior) axes during maximum phase. Tumour	

motion is most limited in this phase, with many cases showing minimal or no displacement, particularly in the Y and Z directions.

	69
Figure 4.3	Boxplot of tumour motion in X (lateral), Y (superior-inferior) and Z (anterior-posterior) axes during minimum phase. The Y-axis exhibits the highest variability and maximum values, reflecting greater respiratory-induced displacement during exhalation.	69
Figure 4.4	Bar graph with $\pm 5\%$ percentage error bars showing the distribution of interfraction motion displacements across longitudinal, lateral, vertical and rotational axes for lung SBRT patients (Patients 1-14), based on average displacements measured over 3 to 5 treatment fractions. Translational displacements are expressed in mm and rotational displacements in degrees ($^{\circ}$).	74
Figure 4.5	Bar graph with $\pm 5\%$ percentage error bars showing the distribution of interfraction motion displacements across longitudinal, lateral, vertical and rotational axes for spine SBRT patients (Patients 15-18), based on average displacements measured over 3 to 5 treatment fractions. Translational displacements are expressed in mm and rotational displacements in degrees ($^{\circ}$).	75
Figure 4.6	Scatter plot of mean interfraction displacement per axis across all 18 patients, with an expanded view focusing on displacement values from 0 mm to 20 mm. The red dotted line indicates the AAPM TG-142 tolerance thresholds (1 mm or 1°).	82

LIST OF SYMBOLS

Z	Anterior-posterior axis
cm	Centimetre
cm ³	Cubic centimetre
°	Degree (angle)
D ₉₅	Dose received by 95% of the volume
=	Equal to
Gy	Gray (unit of absorbed radiation dose)
>	Greater than
≥	Greater than or equal to
HU	Hounsfield Unit
kg	Kilogram
kV	Kilovolt
kW	Kilowatt
X	Lateral axis
≤	Less than or equal to
D _{max}	Maximum dose
MeV	Mega electron volt
MV	Megavolt
µm	Micrometre
mA	Milliampere
mAs	Milliampere-seconds
mGy	Milligray
mm	Millimetre
mm/pixel	Millimetres per pixel (unit of spatial resolution)
ms	Millisecond

MU	Monitor unit
MU/min	Monitor unit per minute (unit of dose rate)
kVp	Peak kilovoltage
%	Percentage
±	Plus-minus
p	p-value (statistical significance)
n	Sample size
s	Second
ρ	Spearman's rank correlation coefficient
cm ²	Square centimetre
mm ²	Square millimetre
Y	Superior-inferior axis
V	Volt

LIST OF ABBREVIATIONS

3D	Three-dimensional
3D-CRT	Three-dimensional conformal radiation therapy
3DCT	Three-dimensional computed tomography
4D	Four-dimensional
4DCT	Four-dimensional computed tomography
4DCT-A	Amplitude-resorted four-dimensional computed tomography
4DCT-P	Phase-resorted four-dimensional computed tomography
6D	Six-dimensional
AAPM TG	American Association of Physicists in Medicine Task Group
AIP	Average intensity projection
AP	Anterior–posterior
aSi	Amorphous silicon
Ave	Average
BED	Biologically effective dose
BEV	Beam’s-eye-view
CA	California
CBCT	Cone beam computed tomography
CCW	Counterclockwise
CT	Computed tomography
CTDI _w	Weighted computed tomography dose index
CTV	Clinical target volume
CW	Clockwise
DD	Dose difference
DICOM	Digital Imaging and Communications in Medicine
DNA	Deoxyribonucleic acid

DTA	Distance-to-Agreement
FB	Free-breathing
FOV	Field of view
gEUD	Generalised Equivalent Uniform Dose
GTV	Gross tumour volume
HPUSM	Hospital Pakar Universiti Sains Malaysia
HREC	Human Research Ethics Committee
IBM SPSS	IBM Statistical Package for the Social Sciences
ICRU	International Commission on Radiation Units and Measurements
ID	Identification
IGRT	Image-guided radiotherapy
IMRT	Intensity-modulated radiation therapy
Inf	Inferior
ITV	Internal target volume
ITV _{all}	Combined ITV from all respiratory phases
ITV _{all+slow}	Combined ITV from all phases plus slow CT
JEPeM	Jawatankuasa Etika Penyelidikan Manusia (USM)
JPNRO	Jabatan Perubatan Nuklear dan Radioterapi Onkologi
KS	Kolmogorov–Smirnov test
kV-CBCT	Kilovoltage cone beam computed tomography
kV-OBI	Kilovoltage On-Board Imager
Lat	Lateral
LINAC	Linear accelerator
Lng	Longitudinal
LR	Left-right
Lt Lat	Left lateral
Max	Maximum

Med	Medial
Min	Minimum
MIP	Maximum intensity projection
MLC	Multileaf collimator
MRI	Magnetic resonance imaging
n/a	Not available
NPC	Nasopharyngeal carcinoma
OAR	Organ at Risk
PET/CT	Combination of positron emission tomography and computed tomography
PTV	Planning target volume
QA	Quality assurance
R50%	Ring structure based on 50% isodose PTV coverage
rcCBCT	Respiration-correlated CBCT
ROSEL	Radiosurgery Or Surgery for Early Lung Cancer
Rt Lat	Right lateral
Rtn	Rotation
RTOG	Radiation Therapy Oncology Group
SAD	Source-to-axis distance
SBRT	Stereotactic body radiation therapy
SD	Standard deviation
SGRT	Surface-guided radiation therapy
SI	Superior–inferior
SRS	Stereotactic radiosurgery
SSN	Suprasternal notch
Sup	Superior
SW	Shapiro–Wilk test
TPS	Treatment planning system

TPU	Thermoplastic polyurethane
USM	Universiti Sains Malaysia
v	Version
VMAT	Volumetric modulated arc therapy
Vrt	Vertical
XST	Xsight spine tracking

LIST OF APPENDICES

Appendix A	JEPeM USM Ethical Approval Letter
Appendix B	Histogram of GTV volume distribution across all tumour sites
Appendix C	Raw data of tumour motion in X, Y and Z directions in maximum and minimum phases
Appendix D	Histogram of relative tumour motion in X, Y and Z directions in maximum phase
Appendix E	Histogram of relative tumour motion in X, Y and Z directions in minimum phase
Appendix F	Raw data of translational and rotational displacements of interfraction motion
Appendix G	Histogram of displacement of interfraction motion in 1 st to 5 th fractions in longitudinal axis
Appendix H	Histogram of displacement of interfraction motion in 1 st to 5 th fractions in lateral axis
Appendix I	Histogram of displacement of interfraction motion in 1 st to 5 th fractions in vertical axis
Appendix J	Histogram of displacement of interfraction motion in 1 st to 5 th fractions in rotational axis
Appendix K	Histogram of mean displacement of interfraction motion in translational and rotational axes

**MENILAI AMBANG GERAKAN ANTARA PEMERINGKATAN
DALAM RADIOTERAPI BERPANDU IMEJ (IGRT) UNTUK TEKNIK
“STEREOTACTIC BODY” DALAM RADIOTERAPI (SBRT) PARU DAN
TULANG BELAKANG**

ABSTRAK

Teknik “stereotactic body” dalam radioterapi (SBRT) merupakan pendekatan lanjutan untuk isipadu tumor yang kecil dan memerlukan penyampaian dos yang tepat kerana sifat hipo-pemeringkatan dan dos gradien yang curam. Namun, pergerakan tumor, terutamanya sesaran akibat respirasi, menimbulkan cabaran terhadap ketepatan rawatan. Kajian ini bertujuan untuk menilai ambang gerakan antara pemeringkatan menggunakan tomografi berkomputer alur kon kilovoltan (kV-CBCT) dalam radioterapi berpandu imej (IGRT) bagi kes SBRT paru dan tulang belakang di Hospital Pakar Universiti Sains Malaysia (HPUSM). **Kaedah:** Untuk tujuh kes SBRT paru, gerakan tumor diukur dalam sistem perancangan rawatan Eclipse dengan mengira jarak antara kontur purata isipadu tumor gros (GTV) dan kontur GTV daripada fasa respiratori maksimum dan minimum menggunakan imej simulasi teknik perlahan tomografi berkomputer “4D-gated”. Gerakan antara pemeringkatan ditentukan melalui kV-CBCT dalam 18 pesakit SBRT paru dan tulang belakang dengan menilai sesaran translasi dan perputaran merentasi 3 hingga 5 pemeringkatan rawatan. Purata sesaran tersebut dibandingkan dengan ambang yang dicadangkan oleh AAPM TG-142 (≤ 1 mm/°). **Keputusan:** Gerakan tumor paling ketara berlaku pada paksi superior-inferior (Y) semasa fasa maksimum (purata = 0.3371 ± 0.4043 cm) dan fasa minimum (purata = 0.1205 ± 0.1677 cm). Korelasi yang kuat ($\rho \geq 0.7$) diperhatikan antara gerakan tumor dan isipadu GTV purata dalam kebanyakan paksi, namun tiada hubungan yang

penanda secara statistik ($p > 0.05$). Gerakan antara pemeringkatan tertinggi dicatatkan pada paksi lateral bagi SBRT paru (purata = 22.89 ± 33.75 mm) manakala SBRT tulang belakang menunjukkan sesaran yang lebih stabil, tertinggi pada paksi vertikal (purata = 22.38 ± 27.36 mm). Tiada perbezaan penanda diperhatikan antara pemeringkatan dan teknik simulasi ($p > 0.05$). Nisbah ambang AAPM TG-142 kepada sesaran sebenar ialah sekitar 1:20 bagi sesaran translasi dan hampir 1:1 bagi sesaran perputaran. **Kesimpulan:** Sesaran gerakan antara pemeringkatan melebihi ambang translasi AAPM TG-142, menekankan keperluan kajian lanjut terhadap pengurusan gerakan bagi mengoptimumkan penyampaian rawatan SBRT.

**EVALUATING INTERFRACTION MOTION THRESHOLDS IN
IMAGE-GUIDED RADIOTHERAPY (IGRT) FOR LUNG AND SPINE
STEREOTACTIC BODY RADIOTHERAPY (SBRT)**

ABSTRACT

Stereotactic body radiotherapy (SBRT) is an advanced technique for small tumour volumes that requires precise dose delivery due to its hypofractionated nature and steep dose gradients. However, tumour motion, particularly respiratory-induced displacement, poses a challenge to treatment accuracy. This study aimed to evaluate interfraction motion thresholds using kilovoltage cone-beam computed tomography (kV-CBCT) in image-guided radiotherapy (IGRT) for lung and spine SBRT at Hospital Pakar Universiti Sains Malaysia (HPUSM). **Methods:** For seven lung SBRT cases, tumour motion was measured in Eclipse treatment planning system (TPS) by measuring the distance between contours of average gross tumour volume (GTV) and GTV from maximum and minimum respiratory phases using 4D-gated slow CT simulation images. Interfraction motion was quantified using kV-CBCT across 18 lung and spine SBRT patients, evaluating translational and rotational displacements over 3 to 5 treatment fractions. The mean interfraction displacements were evaluated against the AAPM TG-142 recommended thresholds (≤ 1 mm/°). **Results:** Tumour motion was highest in the superior-inferior (Y) direction during both maximum (mean = 0.3371 ± 0.4043 cm) and minimum (mean = 0.1205 ± 0.1677 cm) phases. A strong correlation ($\rho \geq 0.7$) was observed between tumour motion and average GTV volume in most axes but the relationships were not statistically significant ($p > 0.05$). Interfraction displacement was highest in the lateral axis for lung SBRT (mean = 22.89 ± 33.75 mm) while spine SBRT showed more stable displacements, with the highest

in vertical axis (mean = 22.38 ± 27.36 mm). No significant differences in displacement were observed across fractions and between simulation techniques ($p > 0.05$). The ratio of AAPM TG-142 threshold to actual displacement was approximately 1:20 for translational displacement and nearly 1:1 for rotational displacement. **Conclusion:** Interfraction motion displacements exceeded AAPM TG-142 translational threshold, highlighting the need of further study for motion management to optimise SBRT delivery.

CHAPTER 1

INTRODUCTION

1.1 Study Background

Cancer is one of the world's leading causes of death, with approximately 9.7 million deaths reported in 2022 (Ferlay et al., 2024). Among all cancer types, lung cancer accounted for the highest global incidence and mortality rates in 2022 (Bray et al., 2024). As a major global health challenge, cancer treatment options include bone marrow transplantation, hormone therapy, surgery, chemotherapy, targeted therapy, immunotherapy and radiotherapy (National Cancer Institute, 2024). Among these, radiation therapy is important, especially for tumours that are surgically inaccessible or require precise targeting (Vaidya, 2021).

The radiotherapy process involves a comprehensive workflow, encompassing patient data acquisition, imaging simulation, treatment planning, quality assurance (QA), treatment delivery and follow-up care. An essential step in this workflow is computed tomography (CT) simulation, where patient positioning, immobilisation and image acquisition are performed for precise tumour and organ delineation. Stereotactic body radiotherapy (SBRT) commonly employs slow CT and four-dimensional CT (4DCT). Slow CT captures an averaged image over multiple breathing cycles while 4DCT segments images by respiratory phase, enhancing the accuracy of target delineation and dose calculation (Dumas et al., 2020; Gallegos, 2023).

Radiotherapy treatment planning techniques are classified into forward planning and inverse planning techniques. SBRT use inverse planning technique, where the treatment planning system (TPS) optimises dose delivery based on predefined constraints. SBRT is a highly precise treatment planning technique that

delivers high doses per fraction (6–30 Gy) over 1 to 5 fractions, unlike three-dimensional conformal radiation therapy (3D-CRT) which uses smaller doses (1.8–3 Gy) across 10 to 30 fractions (Benedict et al., 2010). As illustrated in Figure 1.1, lung 3D-CRT plan exhibits broader coverage while lung SBRT provides a highly conformal dose distribution with steep dose fall-off (Ohtaki et al., 2019).

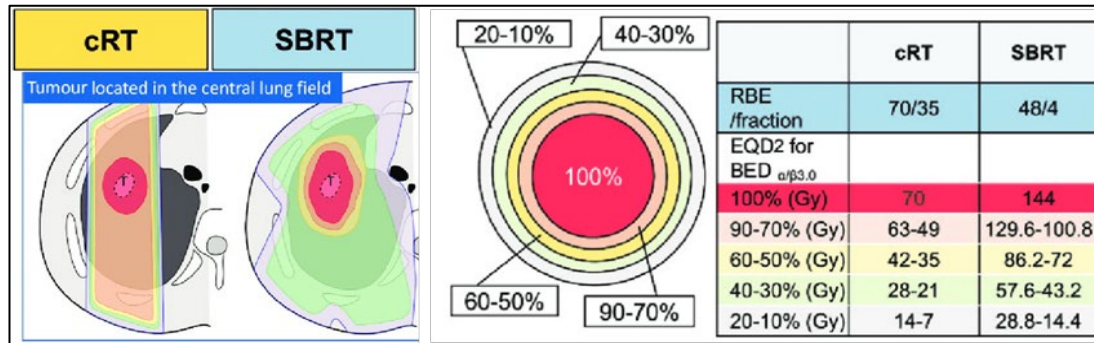


Figure 1.1 Comparison of dose distribution between 3D-CRT and SBRT treatment planning techniques for lung treatment. The SBRT plan demonstrates a steeper dose fall-off than the 3D-CRT plan. (Adapted from Ohtaki et al., 2019)

SBRT also utilises non-coplanar beam arrangements to deliver ablative dose to the target while sparing the surrounding healthy tissues (Seha, 2023). This technique is particularly beneficial for small, well-defined tumours in sites such as the lungs and spine. Since SBRT relies on accurate tumour localisation, managing respiratory motion becomes a critical aspect of the treatment process to maintain precise targeting accuracy.

However, tumour motion between treatment sessions, known as interfraction motion, remains a challenge. Interfraction motion arises due to factors such as respiratory-induced shifts and physiological variations, potentially leading to discrepancies between planned and actual dose delivery. To mitigate this issue, SBRT integrates image-guided radiotherapy (IGRT) techniques such as kilovoltage cone beam computed tomography (kV-CBCT) to obtain real-time images before each

treatment session (Grégoire et al., 2020). IGRT enables precise localisation, reducing radiation exposure to critical organs like the heart, oesophagus, lungs and spinal cord during SBRT treatment (Seha, 2023).

Patient positioning verification in SBRT relies on translational and rotational alignment to ensure accurate tumour targeting. Translational errors refer to shifts in the patient's position along lateral (X), superior-inferior (Y) and anterior-posterior (Z) axes while rotational errors involve angular deviations around these axes (roll, pitch and yaw). SBRT employs kV-CBCT to assess and correct both translational and rotational discrepancies before each treatment session by adjusting the patient's position on the treatment couch. A study by Graadal Svestad et al. (2019) found that using kV-CBCT guidance and patient immobilisation in spine SBRT resulted in high patient positioning accuracy, as evidenced by smaller translational (0.5 mm to 0.6 mm) and rotational (0.3°) errors compared to the larger errors observed without kV-CBCT (0.7 mm to 1.0 mm and 0.4° to 0.7°) (Graadal Svestad et al., 2019).

Despite these advancements, there is no standardised threshold for acceptable interfraction motion in lung and spine SBRT treatment. The American Association of Physicists in Medicine Task Group 142 (AAPM TG-142) report recommends that the tolerance of positioning, repositioning and coincidence of imaging and treatment coordinates should be less than or equal to 1 mm (Klein et al., 2009). However, a gap remains in the standardised thresholds for interfraction motion, particularly in lung SBRT, where respiratory-induced tumour movement introduces complex challenges that often exceed AAPM TG-142's tolerance recommendations (Keall et al., 2006). In contrast, spine SBRT is less influenced by respiratory motion but still demands strict motion control due to the proximity of critical structures like the spinal cord

(Guckenberger et al., 2023). Therefore, a better-defined limit for interfraction motion in lung and spine SBRT treatment is greatly needed in practice to ensure treatment accuracy and safety.

To address this gap, the aim of this study is to evaluate and establish tolerance thresholds for interfraction motion in lung and spine SBRT, using kV-CBCT data to determine allowable motion while maintaining treatment accuracy. This research will contribute critical data to refine clinical guidelines for interfraction motion, improving targeting accuracy, minimising damage to healthy tissue and ultimately enhancing patient outcomes for SBRT.

1.2 Problem Statement

In radiotherapy, achieving precise patient positioning is essential for the safe and effective delivery of treatment. This requirement becomes even more critical in high-precision treatments such as SBRT, which involves delivering high doses in a limited number of fractions. Misalignment between a patient's position during CT simulation and treatment sessions can lead to dose discrepancies, especially in SBRT, where precise alignment is crucial (Benedict et al., 2010). In addition, tumour motion such as respiratory-induced motion can be unpredictable, leading to patient-specific tumour displacement and increasing the risk of dose inaccuracies. AAPM TG-76 reports that lung tumour motion can reach up to 18.5 mm (Keall et al., 2006). If not properly accounted for, this motion may result in target underdosage or unintended irradiation of adjacent healthy tissues, thereby compromising treatment efficacy and patient safety.

The issues that arise from the complexity of SBRT and tumour motion are significant because precise dose delivery is critical due to the high radiation doses

delivered in fewer fractions in lung and spine SBRT. According to Guckenberger et al. (2023), SBRT requires steep dose gradients and highly precise dose delivery to ensure the tumour is fully covered while protecting critical structures like the spinal cord. This is especially important in spine SBRT which requires accurate targeting to help prevent radiation-induced myelopathy, plexopathy and myositis (Guckenberger et al., 2023). Furthermore, the potential for misalignment and unpredictability in motion leads to potential issues in dose distribution, which may result in either underdosing the tumour or overdosing surrounding healthy tissues (Boria et al., 2023). These issues address the need to establish tolerance thresholds for the interfraction motion to improve dose accuracy and treatment outcomes in lung and spine SBRT.

In current clinical practice at the Department of Nuclear Medicine, Radiotherapy & Oncology, Hospital Pakar Universiti Sains Malaysia (JPNRO, HPUSM), respiratory gating with a bellows is only employed during CT simulation for planning but not during actual treatment. Additionally, the treatment couch is often angled to optimise beam orientation meanwhile CT simulations and treatment plans are usually acquired without the angled couch. This misalignment between simulation and treatment settings risks compromising dose accuracy and patient safety. Addressing these limitations is essential to enhance SBRT optimisation, ensuring more accurate dose delivery and improved treatment efficacy.

This study aims to evaluate the interfraction motion using kV-CBCT in lung and spine SBRT cases and to assess how often current practice exceeds the acceptable motion thresholds. Establishing an acceptable threshold for interfraction motion can reduce the reliance on advanced technologies that are lacking by providing a clear limit for how much tumour displacement is allowable during the treatment.

1.3 Research Objectives

1.3.1 General Objective

To evaluate interfraction motion using kilovoltage-cone beam computed tomography (kV-CBCT) in stereotactic body radiotherapy (SBRT) treatment technique at Hospital Pakar Universiti Sains Malaysia (HPUSM).

1.3.2 Specific Objectives

1. To measure tumour motion using 4D-gated slow CT simulation images for lung SBRT.
2. To assess displacement of the interfraction motion for tumour volume in lung and spine SBRT using kV-CBCT.
3. To evaluate interfraction motion thresholds using kV-CBCT in SBRT treatment technique with American Association of Physicists in Medicine Task Group 142 (AAPM TG-142) guidelines.

1.4 Significance of Study

Defining tolerance thresholds for interfraction motion in IGRT for lung and spine SBRT is essential for refining patient setup verification and alignment protocols. This study provides data-driven insights to ensure that radiation beams precisely target the tumour. Given that SBRT requires high-dose, hypofractionated radiation with high precision, this study can reduce positional uncertainties by quantifying and defining appropriate tolerance limits, which are critical for maintaining treatment effectiveness.

Furthermore, establishing appropriate tolerance limits enables adaptive corrections, minimising radiation damage to surrounding healthy tissues and reducing

treatment-related toxicity. By improving the accuracy and consistency of tumour targeting, this study contributes to better tumour control while reducing side effects, ultimately enhancing the quality of life for patients undergoing IGRT for SBRT.

The study's findings can serve as a reference for defining clinically relevant interfraction motion thresholds, supporting the refinement of institutional guidelines. By comparing the identified tolerance values with existing standards, particularly the AAPM TG-142 Report, this study ensures that motion management strategies at JPNRO, HPUSM align with best practices. In summary, this study will improve targeting accuracy, minimise damage to healthy tissue and enhance patient outcomes in IGRT for SBRT.

CHAPTER 2

LITERATURE REVIEW

Radiotherapy is a cornerstone of modern cancer treatment, delivering precise, high-dose radiation to eradicate tumours while minimising damage to surrounding healthy tissues. As illustrated in Figure 2.1, the radiotherapy workflow encompasses several critical steps, including patient data acquisition, imaging simulation, treatment planning, QA, treatment delivery and follow-up care (Benabdessadok, 2023; Ramiah and Mmereki, 2024).

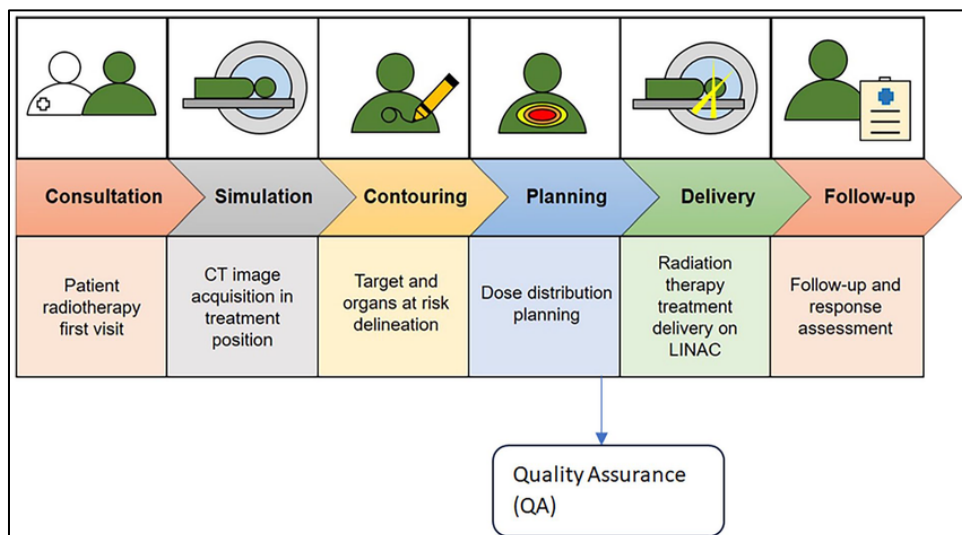


Figure 2.1 Workflow of radiotherapy.

2.1 Tumour Motion

Tumour motion represents a significant challenge in radiotherapy, particularly for thoracic and abdominal sites. It is predominantly caused by physiological processes such as respiration, skeletal muscle contractions, cardiac pulsations and gastrointestinal activity. Among these, respiratory motion is the most influential, affecting nearly all tumours located in the thorax and abdomen (Wu et al., 2024). Respiratory-induced tumour motion is complex and variable, influenced by patient-specific breathing

patterns and anatomical changes during the course of treatment. Tumour and normal tissue volumes may shrink, expand or shift in response to radiation or concomitant therapies, further contributing to motion variability (Keall et al., 2006).

Respiratory-induced tumour motion typically follows a periodic pattern linked to the breathing cycle but can be irregular depending on patient conditions (Keall et al., 2006). The superior-inferior (SI) direction generally exhibits the greatest amplitude of motion, especially for lung tumours located in the lower lobes (Botticella et al., 2021). In contrast, spine tumours exhibit minimal respiratory-induced displacement due to their attachment to the vertebral column (Mizonobe et al., 2023).

In the context of SBRT, where highly conformal beam arrangements are employed to deliver ablative doses to the tumour while sparing adjacent healthy structures, tumour motion poses a particular risk. Unmanaged motion can compromise organ sparing, increase the risk of geographic miss and potentially reduce local control rates (Mizonobe et al., 2023). The clinical consequences of tumour motion are significant. Imaging during simulation may suffer from motion artefacts, leading to inaccurate tumour delineation (den Boer et al., 2021). Additionally, planning target volume (PTV) margins often need to be expanded to account for anticipated motion, inadvertently exposing more normal tissue to high radiation doses (Botticella et al., 2021). Furthermore, motion during beam delivery can cause dosimetric blurring, reducing the effective dose delivered to the tumour (Poolnapol et al., 2022). In high-precision modalities like SBRT, where minimal margins and high doses per fraction are employed, any uncorrected tumour motion can critically impact treatment outcomes.

Studies have reported that lung tumours located in the lower lobes can move up to 18.5 mm superior-inferiorly whereas upper lobe tumours demonstrate significantly

smaller displacements (Keall et al., 2006; Botticella et al., 2021). Respiratory-induced motion of mediastinal lymph nodes has also been documented, typically exceeding 5 mm (Botticella et al., 2021). Conversely, spinal metastases treated with SBRT in prone position using Xsight Spine Tracking demonstrated minimal motion in the superior-inferior (SI) (0.51 ± 0.39 mm) and left-right (LR) (0.37 ± 0.29 mm) directions, although greater displacement was observed in the anterior-posterior (AP) direction (3.43 ± 1.63 mm) (Mizonobe et al., 2023). Despite the minimal movement observed in spinal targets, precision verification through imaging remains critical to avoid geometric uncertainties and maintain the high accuracy required for SBRT. Table 2.1 summarises tumour motion magnitudes for lung and spine based on existing literature.

Table 2.1 Tumour motion magnitudes in lung and spine referring to published work.

Study	Treatment Site	Tumour Motion		Modality Used
		Mean Motion	Range	
(Keall et al., 2006)	Lung (Lower lobe)	18.5 mm (SI)	± 10 mm	Fluoroscopy
	Lung (Middle/Upper lobe)	7.5 mm (SI)	± 2 mm	Fluoroscopy
(Jang et al., 2014)	Lung (Lower lobe)	14.7 mm (3D vector)	-	4DCT + Modified Slow CT
	Lung (Upper lobe)	5.1 mm (3D vector)	-	4DCT + Modified Slow CT
(Botticella et al., 2021)	Lung (Lower lobe, general)	12 ± 6 mm (SI)	-	Fluoroscopy
	Lung (Upper lobe, general)	2 ± 2 mm (SI)	-	Fluoroscopy
	Mediastinal lymph nodes	>5 mm (SI)	-	4DCT

Table 2.1, continued.

Study	Treatment Site	Tumour Motion		Modality Used
		Mean Motion	Range	
(Caines et al., 2022)	Lung	11 mm	-	Phase-resorted 4DCT (4DCT-P)
		13 mm	-	Amplitude-resorted 4DCT (4DCT-A)
		25 mm	-	3DCT
(Mizonobe et al., 2023)	Spine SBRT	0.51 ± 0.39 (SI); 0.37 ± 0.29 (LR); 3.43 ± 1.63 (AP)	-	Xsight spine tracking (XST)

2.2 Computed Tomography (CT) Simulation for Motion Assessment

Precise management of tumour motion is essential in SBRT to achieve high dose conformity and minimise exposure to surrounding healthy tissues. As discussed in Section 2.3, respiratory-induced motion can be substantial, particularly in lower lobe lung tumours, which may exhibit superior-inferior displacements exceeding 10 mm (Botticella et al., 2021; Keall et al., 2006). Unaccounted tumour motion during simulation and treatment can compromise target coverage, increase irradiation of normal structures and reduce treatment efficacy. Consequently, motion assessment during CT simulation plays a critical role in SBRT planning, especially for thoracic and abdominal tumours.

Tumour motion is typically assessed through imaging techniques such as slow CT and 4DCT. These modalities help quantify the tumour's range of motion and support the definition of internal target volumes (ITVs) that account for respiratory variability.

Moreover, motion management strategies such as respiratory gating, which synchronises radiation delivery with specific phases of the breathing cycle, often rely on external surrogates like abdominal pressure belts (Figure 2.2) to track respiratory motion (Botticella et al., 2021). Accurate imaging data from CT simulation is essential to support such techniques.



Figure 2.2 The (A) Abdominal pressure belt and (B) pressure gauge for motion management. (Adapted from Yorke et al., 2015).

2.2.1 Slow CT

Slow CT is an early method used to assess tumour motion by acquiring CT images over multiple breathing cycles with a slow gantry speed. This approach produces time-averaged images that approximate the tumour's motion envelope. Although it provides a blurred representation of the tumour's path, it allows clinicians to generate a composite volume for ITV delineation. It is commonly employed in centres without access to respiratory-correlated imaging or in cases where patients cannot tolerate 4DCT acquisition (Gallegos, 2023).

However, because slow CT lacks temporal resolution, it cannot differentiate between various phases of the respiratory cycle. This limitation increases the risk of missing less frequent but clinically relevant tumour positions, particularly in patients

with irregular breathing patterns (Botticella et al., 2021). For example, a study by Nakamura et al. (2008) showed that 8% of the ITV derived from slow CT was not included in the volume defined by 4DCT in lung tumours located in the upper and middle lobes (Nakamura et al., 2008). As a result, larger margins may be necessary to compensate for the uncertainty, potentially exposing more normal tissue to high-dose radiation. Molla et al. (2016) further compared slow CT with 4D PET/CT and found that the ITV derived from slow CT (mean = $16.3 \pm 17.86 \text{ cm}^3$) was smaller and less accurate than 4D PET/CT (mean = $19.9 \pm 20.50 \text{ cm}^3$), with a greater discrepancy in the cranio-caudal direction ($0.54 \pm 0.61 \text{ cm}$ for slow CT vs. $0.26 \pm 0.33 \text{ cm}$ for 4DCT) (Molla et al., 2016).

Despite these limitations, slow CT remains a useful tool for motion estimation, particularly when combined with 4DCT to compensate for breathing pattern variability. Jang et al. (2014) demonstrated that combining slow CT with 4DCT improved ITV coverage and minimised geometric uncertainties. As shown in Figure 2.3, their findings showed that $\text{ITV}_{\text{all+slow}}$ was significantly larger ($12.5 \pm 8.9 \text{ cm}^3$) compared to ITV_{all} alone ($11.8 \pm 8.3 \text{ cm}^3$), providing better motion representation (Jang et al., 2014).

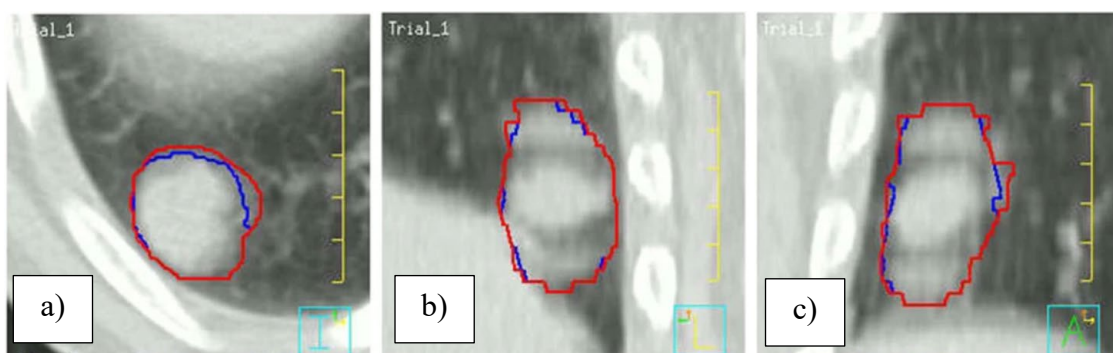


Figure 2.3 The (a) axial, (b) sagittal and (c) coronal views showing the projection of ITV_{all} (blue) and $\text{ITV}_{\text{all+slow}}$ (red) on a modified slow CT scan, comparing between both volumes. (Adapted from Jang et al., 2014)

2.2.2 Four-dimensional CT (4DCT)

4DCT is now the standard imaging technique for assessing respiratory-induced tumour motion in SBRT. 4DCT uses an external respiratory surrogate, such as reflective marker block and abdominal compression belts to record breathing patterns during image acquisition. The data is then retrospectively sorted into time-resolved bins, corresponding to either respiratory phases or amplitudes, resulting in volumetric images that reflect motion throughout the breathing cycle (Botticella et al., 2021; Caines et al., 2022). The gross tumour volume (GTV) is typically contoured in each phase and combined to form ITV, which encompasses the full extent of tumour motion.

Compared to slow CT, 4DCT offers improved motion characterisation, supports the generation of maximum intensity projection (MIP) and average intensity projection (AIP) images (Figure 2.4) and enables the use of mid-ventilation planning techniques (Dumas et al., 2020). This allows for a more accurate definition of internal target volumes while potentially reducing planning margins. Figure 2.3 shows the differences between standard helical CT, MIP and AIP. Caines et al. (2022) demonstrated that 4DCT more accurately represented tumour motion compared to 3DCT, even under irregular breathing conditions. Their study reported median tumour motion errors of 2.5 cm for 3DCT, reduced to 1.1 cm with phase-resorted 4DCT (4DCT-P) and 1.3 cm with amplitude-resorted 4DCT (4DCT-A) (Caines et al., 2022).

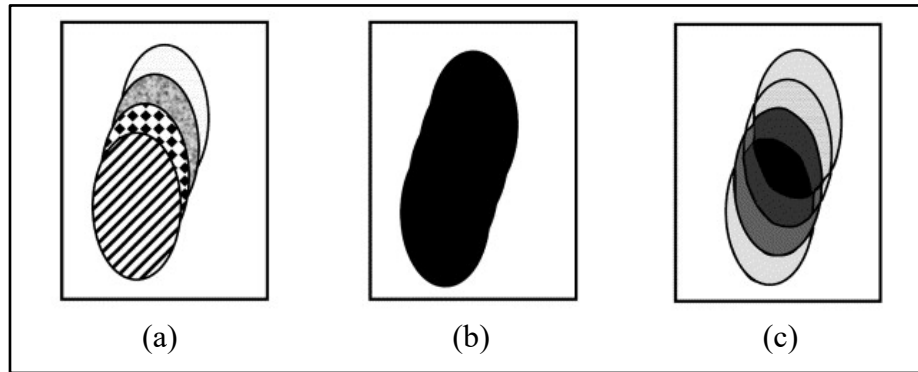


Figure 2.4 Pixel-based intensity projection techniques used in 4DCT, including (a) separate phases of the 4DCT, (b) MIP and (c) AIP. (Adapted from Underberg et al., 2005).

This study incorporates both slow CT and 4DCT to assess tumour motion in patients undergoing lung and spine SBRT. Slow CT is used to approximate motion in patients unable to tolerate 4DCT acquisition or when resources are constrained. In contrast, 4DCT provides detailed temporal resolution of tumour movement and is used to generate data for interfraction motion analysis. While 4DCT improves motion characterisation, uncertainties due to baseline shifts and variable breathing patterns remain, particularly across treatment sessions.

2.3 Radiotherapy Treatment Planning Techniques

Treatment planning is fundamental in ensuring effective and precise radiation therapy. It involves defining target volumes, accounting for organ motion and optimising dose distribution to maximise tumour control while reducing toxicity to organs at risk (OARs). Advances in imaging modalities, contouring techniques and computational algorithms have led to the development of advanced treatment planning methods, ranging from conventional forward planning to highly precise inverse planning approaches (Benabdessadok, 2023).

3D-CRT is a forward planning technique where beam angles, shapes and weights are manually adjusted to achieve an acceptable dose distribution. 3D-CRT utilises field shaping and multiple beam arrangements to improve tumour coverage while minimising exposure to surrounding normal tissue, compared to earlier conventional techniques (Vinod and Hau, 2020). This technique relies heavily on user experience and manual refinement (Grégoire and Mackie, 2011).

With advancements in technology, inverse planning techniques, such as intensity-modulated radiation therapy (IMRT), volumetric modulated arc therapy (VMAT) and SBRT have been introduced. These techniques employ sophisticated optimisation algorithms within the TPS to modulate beam intensity based on predefined constraints. Figure 2.5 compares the beam arrangements of inverse-planned VMAT and forward-planned 3D-CRT (Saito et al., 2023). Unlike forward planning, inverse planning requires specification of desired dose constraints for the target and surrounding OARs as inputs, allowing the TPS to automatically calculate the optimal fluence patterns. This results in highly conformal and customised dose distributions that are challenging to achieve manually, particularly for irregularly shaped or critically located tumours, thereby improving sparing of nearby normal tissues (Grégoire and Mackie, 2011).

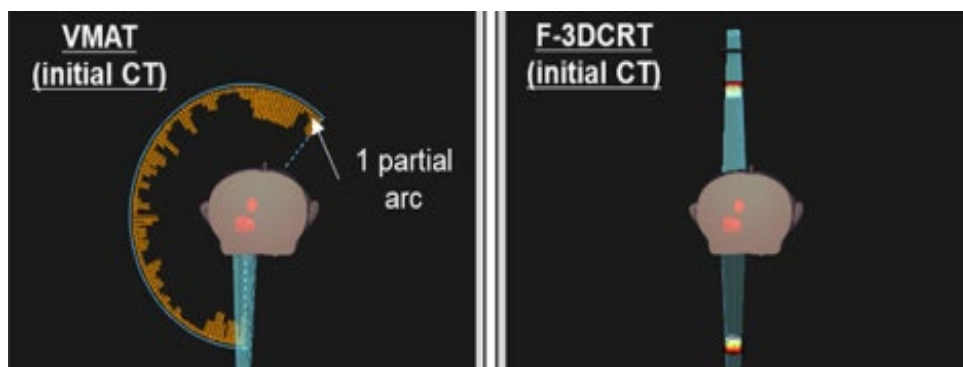


Figure 2.5 Comparisons in the beam arrangements between VMAT (left) and 3D-CRT (right). (Adapted from Saito et al., 2023)

2.3.1 Target Volume Definitions

Accurate delineation of target volumes is fundamental in radiotherapy to ensure the effective delivery of dose to the tumour while minimising exposure to surrounding healthy tissues. The International Commission on Radiation Units and Measurements (ICRU) Report 83 provides standardised definitions of target volumes for IMRT and other advanced techniques where steep dose gradients and high precision are required. As demonstrated in Table 2.2 and Figure 2.6, these definitions serve a specific purpose in addressing uncertainties and ensuring adequate treatment coverage.

Table 2.2 Target volume definitions based on ICRU Report 83. (Adapted from Grégoire and Mackie, 2011)

Volume	Definition
Gross tumour volume (GTV)	The visible or palpable extent of the tumour identified through imaging or examination.
Clinical target volume (CTV)	Includes the GTV plus areas with potential microscopic disease spread and represents the true extent of disease requiring treatment.
Internal target volume (ITV)	Accounts for internal organ motion and changes in shape, size or position of the CTV (e.g., due to respiration or filling).
Planning target volume (PTV)	A geometric expansion of the CTV and ITV to compensate for setup uncertainties and patient movement and ensure the CTV receives the full dose.
Treated volume	The volume enclosed by an isodose surface (often the prescription dose) that adequately covers the PTV.
Irradiated Volume	The volume of tissue receiving a significant dose of radiation, typically defined by the 50% isodose line; includes all tissues exposed.

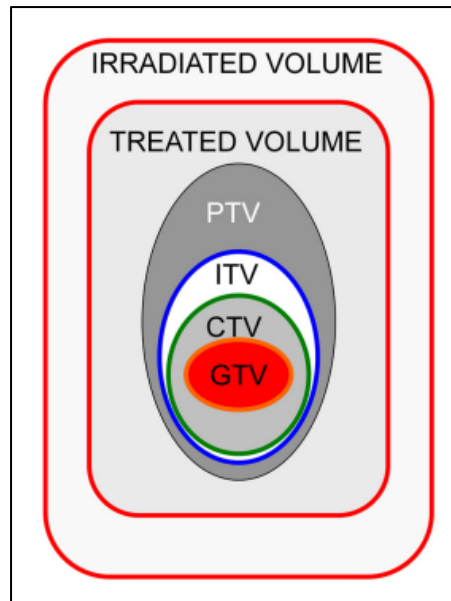


Figure 2.6 Definition of volumes as per ICRU Report 83: GTV in red, CTV in green, ITV in blue, PTV in grey, treated volume and irradiated volume. (Adapted from Grégoire and Mackie, 2011)

2.4 Stereotactic Body Radiotherapy (SBRT)

Among these advanced techniques, SBRT has emerged as a highly precise and effective treatment modality for managing early-stage primary and oligometastatic cancers, particularly in the thoracic, abdominopelvic and spinal regions (Benedict et al., 2010). Unlike conventional fractionated radiotherapy, SBRT delivers high doses per fraction (6 to 30 Gy per fraction) over a limited number of sessions (1 to 5 fractions), resulting in an elevated biological effective dose (BED) that enhances tumour control (Benedict et al., 2010).

While conventional radiotherapy relies heavily on the "4 Rs" of radiobiology, namely repair, redistribution, reoxygenation and repopulation, to explain tumour and normal tissue responses, these mechanisms alone may not fully account for the high efficacy observed with SBRT, as summarised in Table 2.3 (Qiu et al., 2020).

Table 2.3 The 4 Rs of radiobiology in SBRT. (Adapted from Qiu et al., 2020)

Radiobiology	Description
Repair	High single doses overwhelm the repair capacity of tumour cells, leading to lethal damage.
Redistribution	The short course of treatment does not allow both sensitive and insensitive tumour cells redistribution to occur.
Reoxygenation	Less critical in SBRT as the short treatment duration and radiation-induced vascular damage limit its occurrence. Both oxygenated and hypoxic tumour cells are effectively ablated by the high doses delivered in one or a few fractions.
Repopulation	The brief overall treatment time (typically within one week) prevents significant tumour repopulation during therapy.

Beyond the traditional 4 Rs of radiobiology, SBRT introduces additional biological mechanisms, such as secondary cell death, vascular damage and stimulation of antitumour immune responses (Qiu et al., 2020). High-dose radiation not only causes direct tumour cell death through DNA damage but also induces significant vascular injury, leading to secondary tumour cell death due to hypoxia and nutrient deprivation (Song et al., 2021). Importantly, SBRT promotes the release of tumour-associated antigens and pro-inflammatory cytokines, activating systemic immune pathways that can result in delayed but sustained tumour control and suppression of metastasis (Qiu et al., 2020; Song et al., 2021).

The distinct biological effects of SBRT necessitate an equally rigorous technical approach to ensure treatment precision. Delivering very high doses of radiation per fraction over a small number of fractions leaves minimal room for error. This complexity demands a much higher level of precision and accuracy compared to conventional techniques (Benedict et al., 2010). To achieve this, SBRT incorporates stringent immobilisation techniques, frequent image-guided position verification and

advanced respiratory motion management strategies throughout the treatment course (Benedict et al., 2010). These measures enable sub-millimetre targeting accuracy, minimising the risks of tumour underdosing or healthy tissue overdosing caused by patient misalignment or tumour motion (Boria et al., 2023).

Furthermore, to reduce normal tissue toxicity, SBRT requires not only accurate tumour localisation but also the ability to conform high doses tightly to the target with a rapid fall-off in dose outside the target volume (Benedict et al., 2010). Figure 2.7 shows an example of the isodose distribution of a 55 Gy in five fractions of 11 Gy lung SBRT (Kinj et al., 2022).

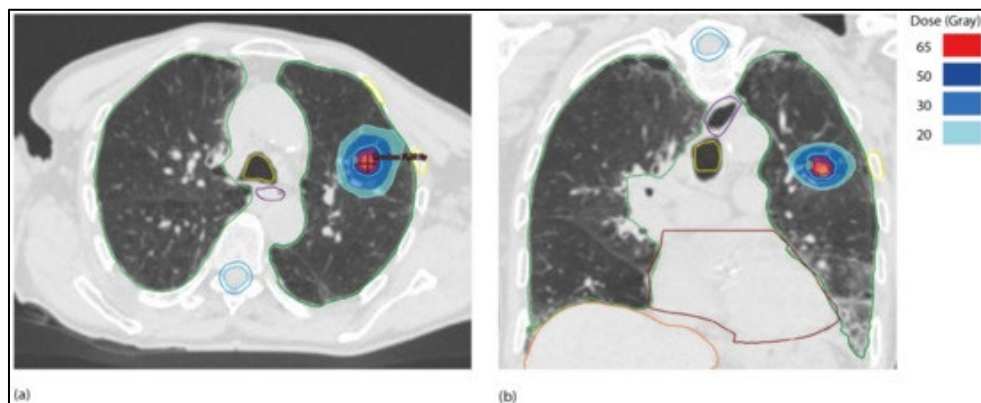


Figure 2.7 Example of the isodose distribution of a 55 Gy in five fractions of 11 Gy lung SBRT. (Adapted from Kinj et al., 2022)

Given the complexity and high stakes of SBRT, a high level of confidence in every phase of the treatment process is critical. This confidence is built through the seamless integration of modern imaging technologies, meticulous simulation, advanced treatment planning and precise treatment delivery (Benedict et al., 2010). A detailed comparison between conventional radiotherapy planning techniques (3D-CRT/IMRT) and SBRT is summarised in Table 2.4.

Table 2.4 Comparison between conventional radiotherapy and SBRT. (Adapted from Benedict et al., 2010).

Characteristic	Conventional Radiotherapy	SBRT
Dose/fraction	1.8 – 3 Gy	6 – 30 Gy
Number of fractions	10 – 30	1 – 5
Target accuracy	May not have a sharp tumour boundary, centimetres margin	Well-defined tumour, millimetres margin
Maintenance of targeting accuracy	Moderately enforced	Strictly enforced
Need for respiratory motion management	Must be at least considered	Highest
Typical use cases	Variety of cancers with larger treatment volumes, palliative care	Lung, spine and other small lesions

2.5 Interfraction Motion

In SBRT, managing interfraction motion is critically challenging due to the high doses and steep dose gradients required for precise tumour targeting. Interfraction motion refers to the change in tumour position between treatment sessions, resulting from variations in patient setup or anatomical shifts. According to the AAPM TG-76 report, interfraction variations are impacted by both respiratory motion and the effectiveness of image-guided and motion management techniques (Keall et al., 2006).

This challenge is particularly significant for lung and spine SBRT. In lung SBRT, interfraction motion can be caused by changes in breathing patterns, tumour regression or anatomical shifts in the thoracic cavity (Li et al., 2021). For spine SBRT, minor deviations in vertebral alignment or immobilisation inconsistencies can result in positional errors exceeding 1 mm or 1°, which may compromise target coverage or increase spinal cord dose (Knybel et al., 2020).

Studies have shown that motion in the superior-inferior, anterior-posterior and lateral directions (Figure 2.8) can reach several millimetres, emphasising the need for precise image guidance and robust immobilisation strategies. Accurately assessing interfraction motion can help to define appropriate PTV margins. Overly large margins may increase the dose to adjacent OARs while small margins risk geographical miss. Therefore, quantifying interfraction variability is essential to maintain the balance between tumour control and normal tissue preservation in SBRT (Grégoire et al., 2020).

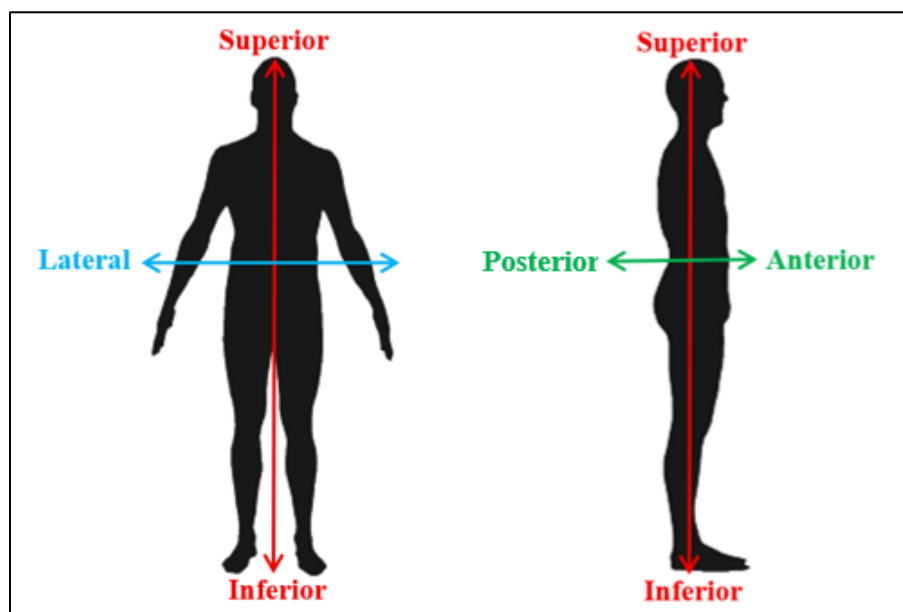


Figure 2.8 Superior-inferior (red), anterior-posterior (green) and lateral (blue) directions.

2.6 Image-guided Radiotherapy (IGRT) Techniques for Motion Management

IGRT is an advanced radiotherapy approach that integrates imaging technology directly into the treatment workflow to enhance tumour localisation and treatment precision. By employing imaging both at the time of treatment planning and during treatment delivery, IGRT ensures accurate patient positioning, optimal radiation dose distribution and reduced setup uncertainties (Hwang et al., 2022). This is especially crucial in techniques such as SBRT, where small margins and high-dose gradients demand sub-millimetre accuracy.

Modern IGRT systems enable adaptive and personalised radiotherapy by incorporating real-time imaging and imaging biomarkers, thereby improving tumour control and reducing radiation exposure to adjacent OARs (Hwang et al., 2022). IGRT enhances the ability to correct for interfraction motion by dynamically aligning patient anatomy with the reference treatment plan before the treatment delivery.

High-resolution and real-time imaging modalities commonly used in IGRT include X-ray imaging, CT and magnetic resonance imaging (MRI). Among these, cone beam computed tomography (CBCT) in LINAC is widely utilised, particularly in SBRT applications, where it plays a pivotal role in both patient setup verification and motion management.

2.6.1 kV-Cone Beam Computed Tomography (kV-CBCT)

kV-CBCT is a widely adopted imaging modality in IGRT, particularly for SBRT, offering sub-millimetre precision in tumour targeting and reducing exposure to surrounding normal tissues (Kavak, 2023). The integration of CBCT systems with linear accelerators (LINACs) allows for on-board volumetric (3D) and four-dimensional (4D) imaging, reducing the need for patient repositioning between imaging and treatment (Hwang et al., 2022). This seamless workflow minimises setup errors and motion uncertainties, making it highly beneficial for treating tumours in anatomically complex or mobile regions such as the lung or spine. Advancements in image reconstruction algorithms, such as iterative reconstruction, further improve CBCT image quality, particularly in regions with significant motion, such as thoracic and abdominal sites (Y. Zhang et al., 2024). These improvements facilitate better visualisation of tumour boundaries and OAR delineation.

A study by Graadal Svestad et al. (2019) highlighted that CBCT significantly enhances positioning accuracy in spine SBRT when combined with appropriate patient immobilisation. Pre-treatment CBCT allows verification of target and bony anatomy, enabling necessary corrections to patient setup (Hwang et al., 2022). This results in high geometric accuracy, permitting the use of smaller PTV margins and reducing radiation exposure to adjacent critical structures (Graadal Svestad et al., 2019).

However, respiratory motion remains a limitation, particularly for tumours near the diaphragm. Differences in deep versus shallow breathing can affect tumour positioning between fractions. This underscores the importance of respiratory motion management strategies, such as breath-hold techniques and respiratory gating, to ensure consistent tumour localisation during treatment. Despite limitations associated with organ motion, CBCT remains the standard for high-precision radiotherapy approaches like SBRT, due to its superior ability to detect and correct for interfractional anatomical changes (Hwang et al., 2022; Kavak, 2023).

2.7 Tolerance Thresholds for Interfraction Motion in SBRT

Given the high precision requirements of SBRT and the steep dose gradients involved, even small deviations in patient or target positioning between treatment sessions can significantly impact clinical outcomes. This necessitates clearly defined tolerance thresholds for interfraction motion to guide corrective actions during IGRT. Therefore, understanding and defining appropriate tolerance thresholds for interfraction motion is essential for both treatment planning and delivery. Guidelines such as those from AAPM TG-142 and findings from recent clinical studies provide practical frameworks for managing this uncertainty.